Mazumdar, S. and Chen, Q. 2009. "A one-dimensional analytical model for airborne contaminant transport in airliner cabins," *Indoor Air,* 19(1), 3-13.

A one-dimensional analytical model for airborne contaminant transport in airliner cabins

Sagnik Mazumdar **Qingyan Chen***

National Air Transportation Center of Excellence for Research in the Intermodal Transport Environment (RITE)
School of Mechanical Engineering, Purdue University, West Lafayette, IN 47907-2088

Abstract: Quick information of airborne infectious disease transmission in airliner cabins is essential to reduce the risk of infection of passengers and crew members. This investigation proposed a one-dimensional analytical model that can predict the longitudinal transmission of airborne contaminants or disease viruses inside an airliner cabin. The model considered both diffusive and convective transport of contaminant in the longitudinal direction of the cabin but assumed complete mixing of contaminants in the cabin cross section. The effect due to recirculation of the cabin air and efficiency of the HEPA filters is also considered in the model. The analytical solution for the one-dimensional contaminant transport model is obtained by using the principle of superposition and the method of separation of variables. The analytical solutions agree well with the Computational Fluid Dynamics (CFD) results. The coupling of a CFD model with the one-dimensional analytical model could capture the impact of local airflow on contaminant transport. This analytical model has been used for analyzing contaminant transport in a 30 row all-economy-class airliner cabin with minimal computing effort.

Keywords: Model, Analytical solution, Contaminant transport, CFD, Airliner cabin

Practical Implications: The paper presents a new one-dimensional analytical model that can provide quick information of global airborne contaminant transmissions in airliner cabins for effective response plans. The model can be used to study the effects of air exchange rates, recirculation, efficiency of the HEPA filters, and longitudinal airflow on airborne contaminant transport in airliner cabins with minimal computing effort.

INTRODUCTION

With close to two billion people traveling each year (Gendreau and DeJohn, 2002), the risk of infectious disease transmission during commercial air travel has become an important public health issue (Mangili and Gendreau, 2005). Airborne contaminant transmissions probably represent the greatest risk for passengers inside aircraft cabins (Mangili and Gendreau, 2005). Airborne transport mechanisms also provide the best explanation to the observed distribution of Severe Acute Respiratory Syndrome (SARS) cases that has occurred in commercial airplanes (Olsen et al., 2003). Other cases of airborne infectious diseases transmitted in airliners in the recent years include tuberculosis, influenza, measles, mumps

*Corresponding author. Tel.: +765-496-7562, Email address: yanchen@purdue.edu

etc. (Musher, 2003; CDC 2006). Investigations on in-flight transmission of tuberculosis showed that the risk of disease transmission should remain within two rows of the contagious passenger (NRC 2002; Jeffrey et al., 1993; Kenyon et al., 1996). But passengers seated as far as seven rows from the source passenger were affected during the SARS incident (Olsen et al., 2003). Insufficient data and incomplete passenger manifestations (Mangili and Gendreau, 2005; Ko et al., 2004) make it difficult to ascertain the probability of disease transmission. Hence the mechanism of disease transmissions within an airliner cabin should be further investigated.

The investigation of airborne disease transmission in cabins can be done by experimental measurements and computer simulations. Although experimental measurements can provide the most realistic information (Zhang et al., 2007a; Zhang et al. 2008; Zhang, T. et al. 2007), such studies are very expensive, time consuming, and difficult. An air cabin simulator would easily cost a million dollar or more and may or may not represent real cabin conditions if the simulator contains only a few rows (Zhang et al., 2007a; Zhang et al. 2008; Zhang, T. et al. 2007). It may not be feasible to conduct experiments in real airliner cabins with passengers and crew on board as the cost of using an aircraft is extremely high. Airliner cabins, no matter whether they are mockups or real ones, are very large spaces. It takes a long time to collect data with meaningful resolutions.

On the other hand, computer simulations using Computational Fluid Dynamics (CFD) can effectively predict airborne contaminant transport in commercial aircraft cabins (Lin et al., 2005a; 2005b). CFD predictions of contaminant transport matched reasonably well with the experimental data (Zhang et al., 2007a; Zhang et al., 2008; Zhang, T. et al., 2007). But a CFD simulation to study contaminant transport for a few minutes in a full length airliner cabin can take a few weeks of computing time even if a computer cluster is used (Mazumdar and Chen, 2008). Thus, CFD has severe limitations in providing quick results, especially real time or faster-than-real-time information of contaminant transport. The time it takes to detect, analyze and implement a system-wide response is critical for an effective response plan (SANDIA website; Policastro and Gordon, 2000). Hence, it is essential to develop an effective model that can provide quick information of airborne contaminant transmissions in airliner cabins.

The fast models available today either assume 1) uniform mixing throughout the airliner cabin or 2) an airliner cabin as a series of uniformly mixed cabin sections with air movement in between sections (Ryan et al., 1988; Ko et al., 2004). Since modern airliner cabins have little airflow in longitudinal direction (NRC 2002) but very strong flow in cross sections, these models are not suitable representations of the cabin environment. For example, the model from Ko et al. accounted for variability due to contaminant source proximity within an airliner cabin based on epidemiological data. Insufficient data and incomplete passenger manifestations generally made it difficult to ascertain the probability of contaminant transmission. Therefore, it is essential to develop an effective model that accurately represents the special airflow features in airliner cabins.

MODEL DEVELOPMENT

The objective of this paper is to develop a model for quick estimates of airborne contaminant transmissions along the longitudinal direction in airliner cabins with reasonable accuracy.

The cabin model

The model development used a fully-occupied, single row of economy-class, twin-aisle cabin as shown in Figure 1. The section shows two linear inlets at the ceiling of the cabin that supply conditioned air to both sides of the cabin. The air was extracted from the two outlets located near the side walls at floor level. The model development replaced the complicated cabin section geometry shown in Figure 1(1) by a simplified one in Figure 1(2). The simplified model used constant properties so that it had a schematic flow configuration shown in Figure 1(3). The F_{inlet} and F_{outlet} represent the flow coming in through the inlets and going out through the outlets, respectively. Moreover, though airliner cabins are expected to have little longitudinal flows, such effects can become significant due to movements inside the cabin (Mazumdar and Chen, 2007). Hence, our transport model incorporates the effect of longitudinal flow (F_L) to study its impact on contaminant transport in the longitudinal direction.

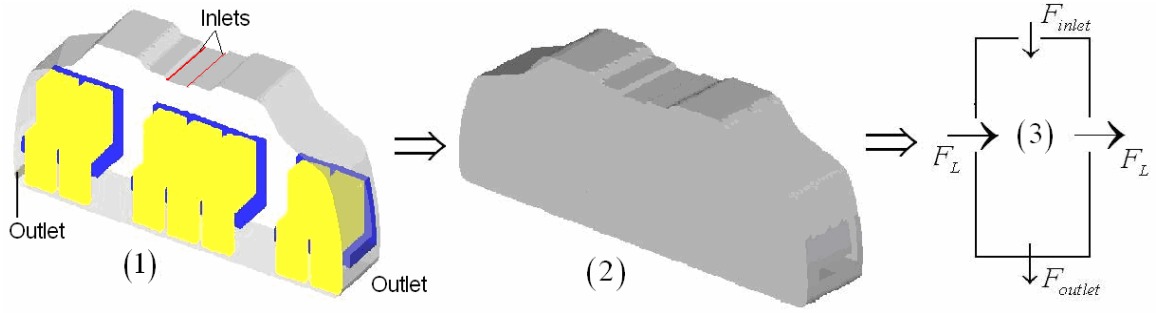

Fig. 1. Schematic representing the simplification of the cabin model

Derivation of the contaminant transport equation

The development of the model considered both diffusive and convective contaminant transports and assumed:

- Uniform contaminant distribution in the cabin cross section due to high air exchange rates and hence contaminant transport is one-dimensional
- Constant density of air (ρ) due to small variations of air temperature and pressure
- The diffusion coefficient of the contaminant (Γ) and the longitudinal velocity (V_L) of air flow to be constant
- The infectious disease viruses to be a gaseous contaminant, as supported by Memarzadeh and Jiang (2000), Seymour (2001) and Ignatius et al. (2004)

Then the one-dimensional contaminant transport equation for a small cabin segment of length *dx* is (Fig. 2):

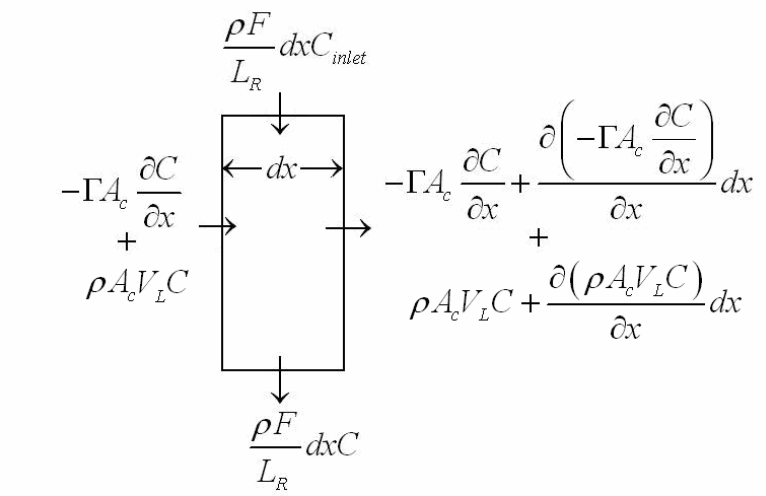

Fig. 2. Contaminant balance in a cabin section with a length of *dx*

$$\overbrace{\rho A_c dx \frac{\partial C}{\partial t}}^{\text{Rate of change}} = \overbrace{-\Gamma A_c \frac{\partial C}{\partial x} - \left[-\Gamma A_c \frac{\partial C}{\partial x} + \frac{\partial\left(-\Gamma A_c \frac{\partial C}{\partial x}\right)}{\partial x} dx\right]}^{\text{Diffusion}} + \underbrace{\rho A_c V_L C - \left[\rho A_c V_L C + \frac{\partial \rho A_c V_L C}{\partial x} dx\right]}_{\text{Convection}} + \underbrace{\frac{\rho F}{L_R} dx C_{inlet}}_{\text{Flow in through inlets}} - \underbrace{\frac{\rho F}{L_R} dx C}_{\text{Flow out through outlets}} \quad (1)$$

where:

L_R = Pitch of each row, m
A_c = Cross section area of the cabin, m^2
C_{inlet} = Contaminant concentration from the inlet, kg/kg_{air}
F = Flow rate per row, m^3/s

Usually, the flow rates are specified by L/s per passenger. Then,

$$\frac{F}{L_R} = \frac{RN_R}{1000 L_R} \quad (2)$$

where:

R = Flow rate in L/s per passenger
N_R = Number of passengers in each row

The resulting equation becomes:

$$\frac{\partial C}{\partial t} = D\frac{\partial^2 C}{\partial x^2} - V_L\frac{\partial C}{\partial x} - \lambda\left(C - C_{inlet}\right) \tag{3}$$

where $D(=\frac{\Gamma}{\rho})$ is the modified diffusion coefficient and $\lambda = \frac{RN_R}{1000 A_c L_R}$

With a contaminant source of S_φ (kg/s) at L_1 released from t=0 to t = t_0, the cabin section is divided into two flow domains with the contaminant source split into $S_{\varphi 1}$ and $S_{\varphi 2}$ representing fractions of the contaminant going to domains 1 and 2, respectively. The contaminant transport equation can then be solved for the two domains as shown in Fig. 3.

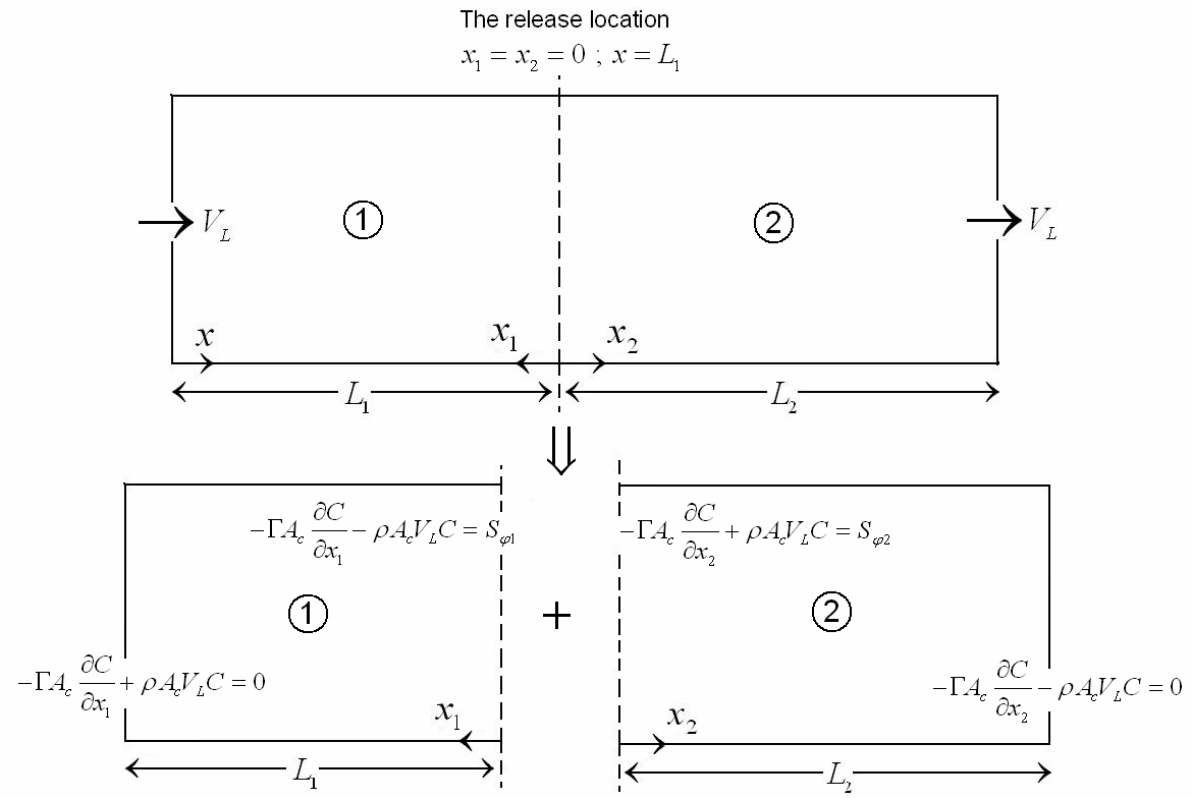

Fig. 3. Schematic of the flow domains

By using the principle of superposition and the method of separation of variables (Carslaw and Jaeger, 1959; Ozisik, 1968; Powers, 2006) the contaminant concentration, C, inside the domain for $x \le L_1$ at $t \le t_0$ will be:

$$C = C_{inlet} + A_{L_1} e^{m_1(L_1 - x)} + B_{L_1} e^{m_2(L_1 - x)} + a_0 e^{-\beta_0^2 t} + 2 \sum_{n=1}^{\infty} a_n \cos\left[\alpha_n \left(L_1 - x\right)\right] e^{-\beta_n^2 t} \quad \text{if } V_L = 0$$

$$= C_{inlet} + A_{L_1} e^{m_1(L_1 - x)} + B_{L_1} e^{m_2(L_1 - x)} + 2\, e^{\frac{V_L}{2D}} \sum_{n=1}^{\infty} a_n \cos\left[\alpha_n \left(L_1 - x\right)\right] e^{-\beta_n^2 t} \quad \text{if } V_L \neq 0 \qquad (4a)$$

and for $x \geq L_1$:

$$C = C_{inlet} + A_{L_2} e^{m_1(x - L_1)} + B_{L_2} e^{m_2(x - L_1)} + a_0 e^{-\beta_0^2 t} + 2 \sum_{n=1}^{\infty} a_n \cos\left[\alpha_n \left(x - L_1\right)\right] e^{-\beta_n^2 t} \quad \text{if } V_L = 0$$

$$= C_{inlet} + A_{L_2} e^{m_1(x - L_1)} + B_{L_2} e^{m_2(x - L_1)} + 2\, e^{\frac{V_L}{2D}} \sum_{n=1}^{\infty} a_n \cos\left[\alpha_n \left(x - L_1\right)\right] e^{-\beta_n^2 t} \quad \text{if } V_L \neq 0 \qquad (4b)$$

The procedure for finding the coefficients (*A, B, a, α, β*) is derived in Appendix A. Moreover modern airplanes recirculate 50% of the total air after passing them through high efficiency particulate air (HEPA) filters (BOEING website). The contaminant concentration coming in through the inlets (C_{inlet}) at time t will depend on the fraction of air recirculated (F_R) and efficiency of the HEPA filters (E_{HEPA}):

$$C_{inlet}\Big|_t = F_R \quad \frac{100 - \mathrm{E}_{\mathrm{HEPA}}}{100} \quad \frac{\int_0^{L_1 + L_2} C dx}{\left(L_1 + L_2\right)}\Bigg|_{t - t_{rec}} \qquad (5)$$

t_{rec} is the time taken by the air going out through the outlets to recirculate back to the cabin. Furthermore, the contaminant concentration for $t \geq t_0$ is:

$$C = C_{inlet} + A e^{m_1 x} + B e^{m_2 x} + b_0 e^{-\beta_0^2 (t - t_0)} + 2 \sum_{m=1}^{\infty} b_m \cos\left(\alpha_m x\right) e^{-\beta_m^2 (t - t_0)} \quad \text{if } V_L = 0$$

$$= C_{inlet} + A e^{m_1 x} + B e^{m_2 x} + 2\, e^{\frac{V_L}{2D}} \sum_{m=1}^{\infty} b_m \cos\left(\alpha_m x\right) e^{-\beta_m^2 (t - t_0)} \quad \text{if } V_L \neq 0 \qquad (6)$$

Please note that the modified diffusion coefficient of the contaminant *D* is unknown.

Determination of the modified diffusion coefficient, D

This investigation used CFD simulations to determine the modified diffusion coefficient *D* of the contaminant, because CFD can effectively predict contaminant transmission for diverse indoor environments (Spengler and Chen, 2000) and in commercial aircraft cabins (Lin et al., 2005a; 2005b). This study used CFD program FLUENT as it was validated with experimental data by Zhang *et al.* (2007a; 2008). The turbulence model used is the Re-Normalization Group (RNG) *k-ε* model (Yakhot and Orszag, 1986) as it was successful in modeling diverse indoor airflows (Chen, 1995; Zhang et al., 2007b). The numerical scheme used the second-order upwind scheme and the SIMPLE algorithm with a segregated steady state solver.

This investigation used a single row cabin model shown in Fig. 4 to calculate the *D*. All the seats are occupied by box-shaped manikins representing the passengers since they were sufficient for the study of global airflow (Topp et al., 2002). Grid independence studies confirmed that a grid size of 6 cm was appropriate (Chen, 2007). The calculation of the *D* has the following three steps:

- Step 1: To compute the steady airflow field using periodic boundary conditions for faces 1 and 2.
- Step 2: To compute the contaminant concentration at face 2, C_2, by setting $C=C_0$ for face 1 and $dC/dx = 0$ (Outflow condition) for face 2 and assuming $C_{inlet}=0$.
- Step 3: To repeat step 2 to obtain the contaminant concentration C_1 at face 1 by setting $C=C_0$ for face 2 and $dC/dx = 0$ for face 1. The C_1 and C_2 may not the same because of a small longitudinal flow (V_L).

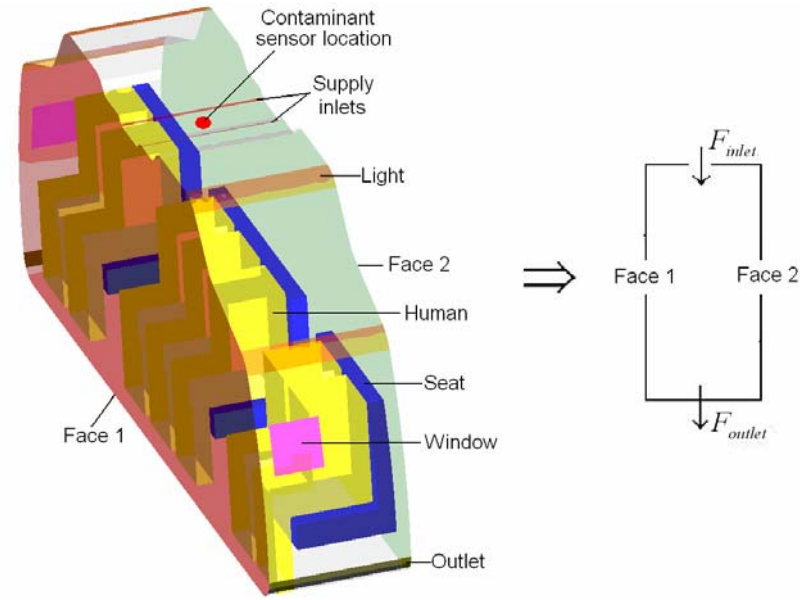

Fig. 4. Schematic of the twin aisle cabin model used for analyses

The solution of the contaminant transport equation, Eq. (3), under steady state is:

$$C_1 = \frac{C_0\left(m_2 - m_1\right)e^{(m_1+m_2)L_R}}{\left(m_2 e^{m_2 L_R} - m_1 e^{m_1 L_R}\right)} \;;\; C_2 = \frac{C_0\left(m_2 - m_1\right)}{\left(m_2 e^{m_1 L_R} - m_1 e^{m_2 L_R}\right)} \tag{7}$$

where:

$$m_1 = \frac{V_L + \sqrt{V_L^2 + 4\lambda D}}{2D} \;;\; m_2 = \frac{V_L - \sqrt{V_L^2 + 4\lambda D}}{2D}$$

By replacing C_1 and C_2 obtained in the three-step approach in Eq. (7), the modified diffusion coefficient, D, can be obtained. Since CFD is used to calculate D, this model indirectly captures the effect of increased diffusion due to increased turbulence with higher ventilation rates that was considered in the previous models (Ko et al., 2004; Ryan et al., 1988).

MODEL PERFORMANCE

The performance of the one-dimensional analytical model for steady-state contaminant transport was evaluated by comparing it with CFD simulation results for a ten-row cabin section as shown in Fig. 5. Row geometry for CFD is as shown in Fig. 4. The CFD simulations assumed contaminants released from the mouths of the two passengers seated in the fifth row (5A and 5E). The contaminant was released at a continuous rate of 1.0 X 10^{-6} kg/s per person. The supply airflow rate was 10 L/s per passenger (Mazumdar and Chen, 2008). The temperatures for the interior enclosure obtained from on-site measurements (Mazumdar and Chen, 2008) are shown in Table 1. Periodic boundary conditions were used at the ends for simulating the airflow and contaminant concentrations. Since previous studies observed that the optimal location for placement of contaminant detection sensors is at the center of the cabin ceiling as shown in Fig. 4 (Mazumdar and Chen, 2008; Zhang, T. et al., 2007), our analytical calculations are compared with the CFD results of contaminant concentrations at the sensor location.

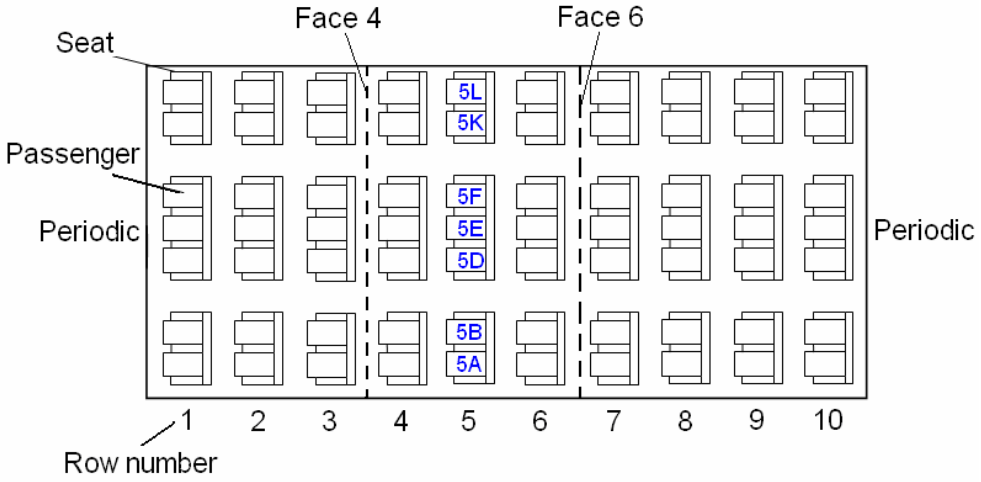

Fig. 5. Schematic of the twin-aisle, ten-row cabin section

Table 1. Thermal boundary conditions used for the cabin section

Supply air	19.5 ^{o}C	Floor under side seats	23 ^{o}C
Ceiling within inlets	25 ^{o}C	Windows	13 ^{o}C
Ceiling (from inlets to lights)	23 ^{o}C	Passengers	30.3 ^{o}C
Side walls	18 ^{o}C	Lighting	12.5 W/row
Floor under center seats	24 ^{o}C		

Figure 6(a) compares the analytical prediction of contaminant concentrations with the CFD results obtained for contaminant released from passengers 5A (near window seat) and 5E (near middle seat). In general, the analytical prediction of longitudinal contaminant transport agrees well with the CFD results. But at the row where the contaminant was released from passenger 5E, the model under-predicted the contaminant concentration at the sensor location. The location was in the downstream of the thermal plume generated by passenger 5E and hence local flow effects were prominent. The figure also shows that the cross-sectional averaged contaminant concentrations ($C_{CSaverage}$) are close to those at the sensor locations except for row 5 & 6. Hence the uniform mixing assumption in a cross section used in the one-dimensional model is acceptable. The asymmetrical contaminant transport in the longitudinal direction due to release at 5E was not correctly predicted. This is again attributed to the effects of local flow.

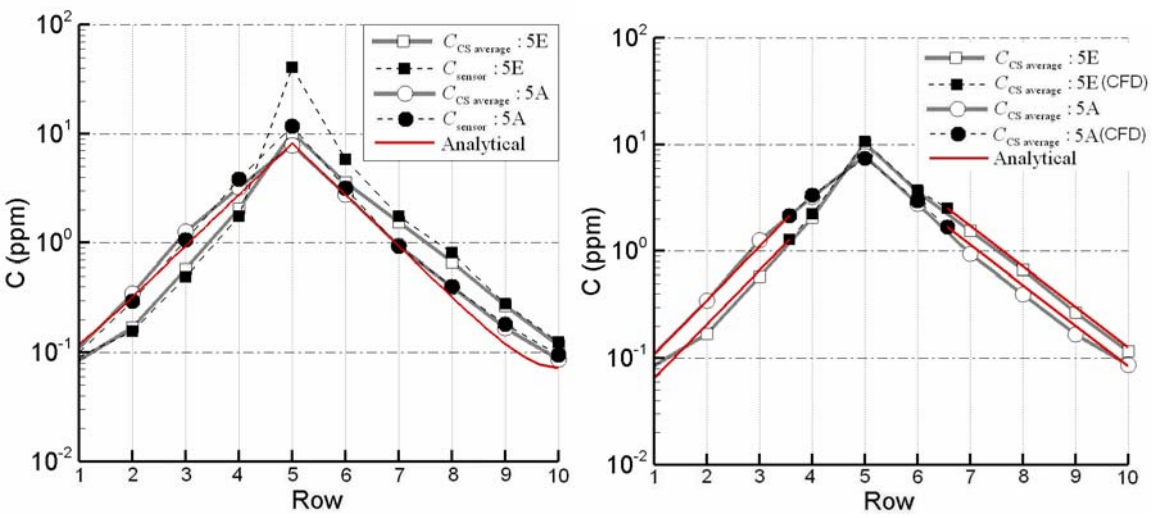

(a) (b)

Fig. 6. Comparison of contaminant concentrations along the longitudinal direction, (a) between the analytical model and the CFD model and (b) between the coupled CFD and analytical model and the CFD model

To capture the effects of local flow, this investigation used a combined CFD and one-dimensional analytical model. CFD was used to calculate local contaminant transport for rows 4-6 and the analytical model for the rest of the cabin. The coupling procedure is as follows:

- Step 1 was to use CFD to compute the steady airflow field using periodic boundary conditions at faces 4 & 6 (Fig. 5)
- Step 2 was to compute the averaged contaminant concentrations (C_{Face4} and C_{Face6}) using outflow conditions at faces 4 & 6
- Step 3 was to use C_{Face4} and C_{Face6} as inputs to the analytical model to obtain the contaminant transport in the rest of the cabin (rows 1-3 and 7-10).

Figure 6(b) shows that the averaged contaminant concentrations obtained with the coupled CFD and analytical model for contaminants released from passengers 5A and 5E. The results are in excellent agreement with those obtained by CFD for the whole cabin. Clearly, CFD helps the coupled model to capture the local effects while the analytical model is sufficient for longitudinal contaminant transport.

Note that the performance of analytical model is tested with uniform inlet flow conditions and periodic conditions at the end walls. Recent investigation by Mazumdar et al. (2008) revealed that the supply airflow conditions can be highly non-uniform. Figure 7 shows the effect of supply airflow and end wall conditions on the cross-sectional averaged contaminant concentrations inside the ten-row cabin section obtained using CFD. For an airplane with 6 to 7 seats in a row, the total row number is 20-40 rows that will make the end effect even less important. Fig. 7 indicates that the end wall conditions at the 10-row cabin have less influence compared to the non-uniform inlet conditions, which significantly enhance the longitudinal mixing of contaminants. With the non-uniform flow condition from the air supply inlet, the contaminant concentration is much better mixed between rows. As a result, the decay on contaminant concentration for the case shown here is one magnitude order every four rows.

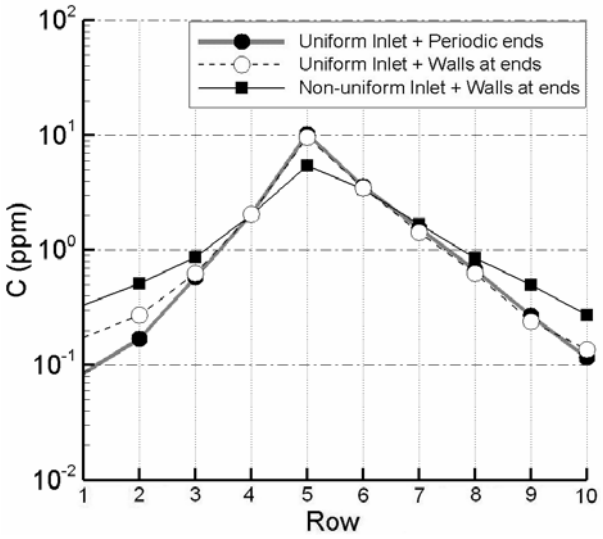

Fig. 7. Effect of inlet flow and end wall conditions on contaminant transport inside the ten-row cabin for contaminant released from passenger 5E

Moreover, the results presented in this paper are for gaseous contaminants. Infectious disease viruses consist of particle size ranging 0.1 to 100 micron. Small particles exhibit gaseous behavior but larger particles behave differently. For large particles, the diffusion properties can vary. This implies that one may have to use several diffusion coefficients for different ranges of particles. In addition, large particles may deposit on the surface much easier than small ones. Different deposition rates should be used for different particle size. The deposition can be modeled by adding a contaminant sink term to the governing transport Eq. 1.

MODEL APPLICATIONS

This section will show some applications of the one-dimensional model for calculating contaminant transport in an all-economy-class commercial airliner cabin of 30 rows with uniform inlet flow conditions. The study assumed an imaginary contaminant released at a continuous rate of 1×10^{-6} kg/s in the cabin. This investigation further assumed that the efficiency of the HEPA filters in the cabin was 100% so the contaminant was not recirculated back to the cabin.

Figure 8(a) plots concentration profiles in the cabin at t = 2, 5, and 10 minutes and at steady state. The results show that the contaminant transport along the longitudinal direction was slow and had a very high decay rate. In two minutes, the contaminant could be dispersed by eight rows in either direction with eight orders of magnitude decay. The contaminant distribution became quasi-steady state in no less than ten minutes. Even at the steady state, the decay from the middle of the cabin to either end was six orders of magnitude. This model provides useful information about the contaminant transports. This study has also used CFD simulation to calculate the contaminant transport for two minutes of real time. The computation took 4 weeks of computing time with a 16-processor computer cluster (Mazumdar and Chen, 2008). The analytical model can provide instant results.

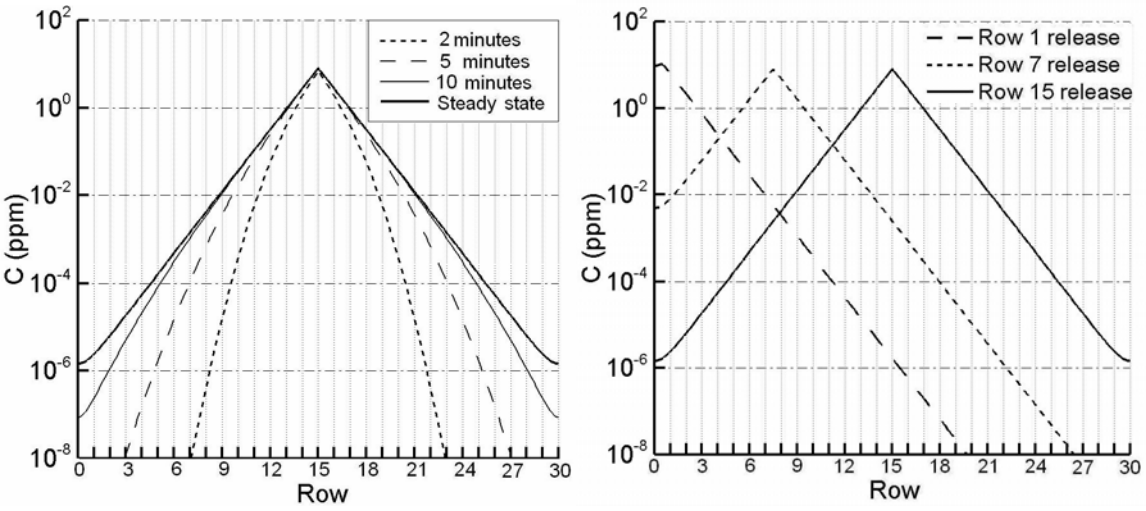

Fig. 8. Contaminant transport inside a 30-row airliner cabin with a continuous contaminant source, (a) released at row 15 and (b) released at rows 1, 7 and 15

Figure 8(b) presents the contaminant concentration profiles at steady state for releases at rows 1, 7 and 15, respectively. The profiles look the same but shifted with the source locations. A contaminant released in row 1 would contaminate only half of the passengers than that in row 15.

In addition to the source strength, the duration of a release is also an important parameter that governs the risk associated with longitudinal contaminant transport. Figure 9 shows the contaminant concentration profiles in the cabin with a strong source of 100×10^{-6} kg/s released for five minutes. The profiles are plotted at t = 5, 10, 20 and 30 min respectively after the contaminant was released. The environmental control system of the cabin sharply reduces the contaminant concentration in the beginning but slows down later. The concentration reduction is not proportionate with time. Roughly, the peak contaminant concentration reduced by two orders of magnitude every ten minutes.

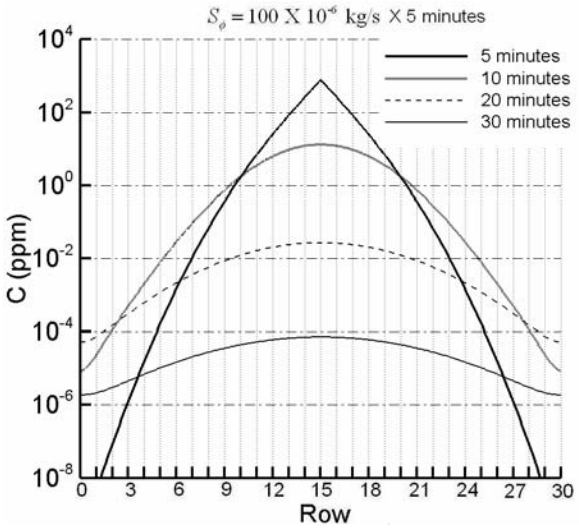

Fig. 9. The effect of release duration of a contaminant transport in a cabin

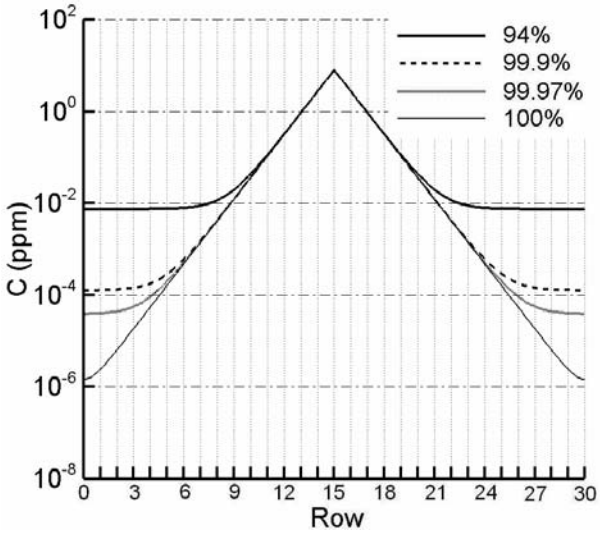

Fig. 10. The effect of filter efficiency on contaminant transport

Another important parameter that can play an important role in contaminant transport is the efficiency of the HEPA filters. In general, HEPA filters used in commercial airliners have a particle removing efficiency of 99.9 percent at 0.3 microns (BOEING website), but it can be as low as 94 percent. Figure 10 shows the effect of filter efficiency for a continuous contaminant release rate of 1×10^{-6} kg/s in row 15. The cabin used 50 percent of outside air and the other 50 percent of recirculated air. When the filter efficiency was at 94 percent, the contaminant concentration could only be reduced by three orders of magnitude from its peak. A filter with such a low efficiency would not protect the passengers who sit far away from the source. With a 99.9% efficient filter as it should have, the reduction was five orders of magnitude from its peak. Further increase of the filter efficiency may be difficult but its effectiveness was also not very evident as shown in Fig. 10.

Please note that all the above results were obtained assuming no longitudinal flow inside the cabin. Though airliner cabins have little longitudinal flows, the flow could become significant due to passenger and crew movements inside the cabin (Mazumdar and Chen, 2007). By using the 30-row cabin with 100% efficiency HEPA filters, Fig. 11 shows the impact of longitudinal flow on contaminant transport. The γ is the ratio of longitudinal flow over the flow supplied to a row from the environmental control system. The longitudinal flow made the contaminant distribution asymmetrical. The higher the longitudinal flow, the more asymmetric is the contaminant transport.

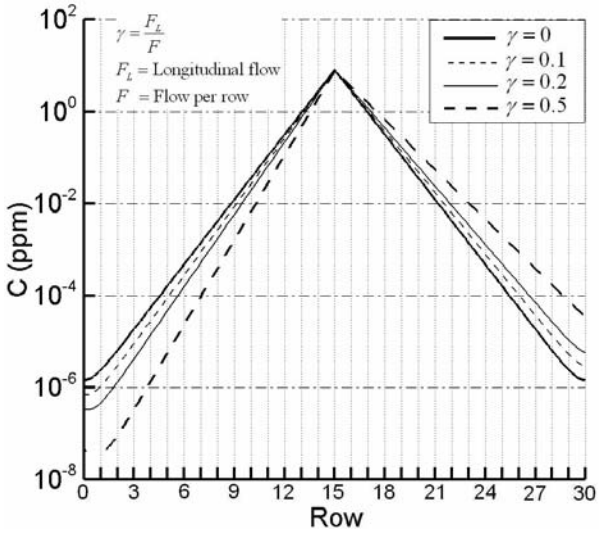

Fig. 11. The effect of longitudinal flow on contaminant transport in a cabin

CONCLUSIONS

This paper presents a one-dimensional analytical model to predict longitudinal transport of airborne contaminants inside an airliner cabin. The model assumes uniform mixing of contaminant in cross sections of the cabin. The model can consider the effects of air exchange rates, recirculation, efficiency of the HEPA filters, and longitudinal airflow on

airborne contaminant transport. The analytical model gives reasonable estimates of longitudinal contaminant transport when compared with CFD results, except in the proximity of the contaminant source. The effects caused by local airflow near the contaminant source on contaminant transport can be addressed by coupling it with a CFD model for the region.

The analytical model has been applied to analyze different scenarios of contaminant transport in an airliner cabin with 30 rows of all-economy-class seats with uniform inlet flow conditions. The results lead to the following conclusions:

- For the cabin investigated, quasi-steady conditions were achieved in approximately ten minutes with a constant contaminant source. The decay of contaminant concentration with a source in the middle of the cabin to either end is six orders of magnitude. Conceivably for other cabins, this result would be different.
- A contaminant released near cabin ends would contaminate only half of the passengers compared to a release near the middle.
- If a contaminant is released in the cabin for five minutes, the peak contaminant concentration reduced by two orders of magnitude every ten minutes.
- When HEPA filter efficiency is 94%, the contaminant concentration could only be reduced by three orders of magnitude from its peak. With a 99.9% efficient filter, the reduction is five orders of magnitude. Further increase of the filter efficiency is not very effective.
- Longitudinal and local airflows can make the contaminant transport asymmetric in the longitudinal direction.

ACKNOWLEDGEMENTS

This project is funded by the U.S. Federal Aviation Administration (FAA) Office of Aerospace Medicine through the National Air Transportation Center of Excellence for Research in the Intermodal Transport Environment under Cooperative Agreement 07-C-RITE-PU. Although the FAA has sponsored this project, it neither endorses nor rejects the findings of this research. The presentation of this information is in the interest of invoking technical community comment on the results and conclusions of the research.

REFERENCES

Carslaw, H.S., and Jaeger, J.C. (1959) Conduction of heat in solids. *Oxford University Press, Amen House, London*.

Chen, Q. (1995) Comparison of different k-ε models for indoor air flow computations. *Numerical Heat Transfer, Part B* 28: 353-69.

Chen, X. (2007) A numerical study on decontaminating unoccupied airliner cabins. M.S. Thesis. Purdue University.

Gendreau, M.A., and DeJohn, C. (2002) Responding to medical events during commercial airline flights. *New England Journal of Medicine* 346(14): 1067-73.

http://www.boeing.com/commercial/startup/passenger.html

http://www.ca.sandia.gov/chembio/facilities_protect/protect/index.html

http://www.cdc.gov/mmwr/. May 18, 2006. Update: Multistate Outbreak of Mumps - United States, January 1-May 2, 2006

Ignatius, T.S.Y., Yuguo, L., Tze, W.W., Wilson, T., Andy, T.C., Lee, J.H.W., Dennis, Y.C.L., and Tommy, H. (2004) Evidence of airborne transmission of the Severe Acute Respiratory Syndrome Virus. *New England Journal of Medicine* 350(17): 1731-39.

Jeffrey, W.M., Cynthia, H., Michael, T.O., and Kristine, L.M. (1993) Exposure to Mycobacterium tuberculosis during air travel. *Lancet* 342: 112-113.

Kenyon, T.A., Valway, S.E., Ihle, W.W., Onorato, I.M., and Castro, K.G. (1996) Transmission of multidrug resistant mycobacterium tuberculosis during a long airplane flight. *New England Journal of Medicine* 334: 933-38.

Ko, G., Thompson, K.M., and Nardell, E.A. (2004) Estimation of tuberculosis risk on a commercial airliner. *Risk Analysis* 24(2): 379-388.

Lin, C.H., Horstman, R.H., Ahlers, M.F., Sedgwick, L.M., Dunn, K.H., Topmiller, J.L., Bennett, J.S., and Wirogo, S. (2005a) Numerical simulation of airflow and airborne pathogen transport in aircraft cabins - Part 1: Numerical simulation of the flow field. *ASHRAE Transactions* 111(1):755-63.

Lin, C.H., Horstman, R.H., Ahlers, M.F., Sedgwick, L.M., Dunn, K.H., Topmiller, J.L., Bennett, J.S., and Wirogo, S. (2005b) Numerical simulation of airflow and airborne pathogen transport in aircraft cabins - Part 2: Numerical simulation airborne pathogen transport. *ASHRAE Transactions* 111(1): 764-68.

Mangili, A, and Gendreau, M.A. (2005) Transmission of infectious disease during commercial air travel. *Lancet* 365: 989-96.

Mazumdar, S. and Chen, Q. (2007) Impact of moving bodies on airflow and contaminant transport inside aircraft cabins. *Proceedings of the 10th International Conference on Air Distribution in Rooms, Roomvent 2007*, Helsinki, Finland: 165.

Mazumdar, S., and Chen, Q. (2008) Influence of cabin conditions on placement and response of contaminant detection sensors in a commercial aircraft. *Journal of Environmental Monitoring*, DOI: 10.1039/b713187a.

Mazumdar, S., Priyadarshana, P.A., Keshavarz, A., Chen, Q., and Jones, B.W. (2008) Flow characteristics from air supply diffusers and their effect on airflow and contaminant transport

inside aircraft cabin. *Submitted to the 11th International Conference on Indoor Air Quality and Climate (Indoor Air 2008)*, Copenhagen, Denmark.

Mermarzadeh, F., and Jiang, J. (2000) Methodology for minimizing risk from air-borne organisms in hospital isolation rooms. *ASHRAE Transactions* 106(2): 733-49.

Mora, L., Gadgil, A.J., and Wurtz, E. (2003) Comparing zonal and CFD model predictions of isothermal indoor airflows to experimental data. *Indoor Air*, 13: 77-85.

Musher, D.M. (2003) How contagious are common respiratory tract infections? *New England Journal of Medicine* 348: 1256-66.

NRC (National Research Council). (2002) The airliner cabin environment and the health of passengers and crew. Washington, DC: *National Academy Press*.

Olsen, S.J., Chang, H.L., Cheung, T.Y., Tang, A.F., Fisk, T.L., Ooi, S.P., Kuo, H.W., Jiang, D.D., Chen, K.T., Lando, J., Hsu, K.H., Chen, T.J., and Dowell, S.F. (2003) Transmission of the severe acute respiratory syndrome on aircraft. *New England Journal of Medicine* 349(25): 2416-22.

Ozisik, M.N. (1968) Boundary value problems of heat conduction. *International Textbook Company, Pennsylvania*.

Policastro, A.J., and Gordon, S.P. (2000) The use of technology in preparing subway systems for chemical/biological terrorism. *APTA Rapid Transit Conference*.

Powers, D.L. (2006) Boundary value problems and partial differential equation. *Elsevier Academic Press*.

Ryan, P.B., Spengler, J.D., and Halpfenny, P.F. (1988) Sequential box models for indoor air quality: application to airliner cabin air quality. *Atmospheric Environment* 22 (6): 1031-1038.

Schaelin, A., Dorer, V., van der Mass, J., and Moser A. (1993) Improvement of multizone model predictions by detailed flow path values from CFD calculation. *ASHRAE Transactions*, 93-7-4: 709-720.

Seymour, M.J. (2001) Practical airflow design and optimization in clean rooms using mathematical modeling. *Flomerics Ltd.* http://www.flomerics.com/flovent/technical_papers/v17.pdf

Spengler, J.D., and Chen, Q. (2000) Indoor air quality factors in designing a healthy building. *Annual Review of Energy and the Environment* 25: 567-600.

Topp, C., Nielsen, P., and Sorensen, D. (2002) Application of computer simulated persons in indoor environmental modeling. *ASHRAE Transactions* 108(2): 1084-89.

Wang, L., and Chen, Q. (2007) Theoretical and numerical studies of coupling multizone and CFD models for building air distribution simulations. *Indoor Air*, 17: 348-361.

Yakhot, V., and Orszag, S.A. (1986) Renormalization group analysis of turbulence. *Journal of Scientific Computing* (1): 3-51.

Zhang, T., Chen, Q., and Lin, C.-H. (2007) Optimal sensor placement for airborne contaminant detection in commercial aircraft cabins. *HVAC&R Research*, 13(5): 683-696.

Zhang, Z., Chen, X., Mazumdar, S., Zhang, T., and Chen, Q. (2007a) Experimental and numerical investigation of airflow and contaminant transport in an airliner cabin mock-up. *Proceedings of the 10th International Conference on Air Distribution in Rooms, Roomvent 2007*, Helsinki, Finland: 171.

Zhang, Z., Zhang, W., Zhai, Z. and Chen, Q. (2007b) Evaluation of various turbulence models in predicting airflow and turbulence in enclosed environments by CFD: Part-2: comparison with experimental data from literature. *HVAC&R Research*, 13(6)*:* 871-886.

Zhang, Z., Chen, X., Mazumdar, S., Zhang, T., and Chen, Q. (2008) Experimental and numerical investigation of airflow and contaminant transport in an airliner cabin mock-up. *Building and Environment*, under review.

Appendix A

$S_{\varphi 1}$ and $S_{\varphi 2}$ represent fractions of the contaminant source S_{φ} going to domains 1 and 2, thus:

$$S_{\varphi} = S_{\varphi 1} + S_{\varphi 2} \tag{A1}$$

The procedure is outlined for domain 2 only as solution methodology is similar for both domains. The boundary condition at x_2=0 assuming a passive contaminant release is:

$$\left.\begin{aligned} -\Gamma A_c \frac{\partial C}{\partial x_2} + \rho A_c V_L C = S_{\varphi 2} \ \text{ at } x_2 = 0 \text{ for } t \le t_0 \\ -\Gamma A_c \frac{\partial C}{\partial x_2} - \rho A_c V_L C = 0 \quad \text{at } x_2 = 0 \text{ for } t > t_0 \end{aligned}\right\} \tag{A2a}$$

$$\Gamma A_c \frac{\partial C}{\partial x_2} + \rho A_c V_L C = 0 \quad \text{at } x_2 = L_2 \tag{A2b}$$

The contaminant is released till t = t_0 and stops after that. The initial contaminant concentration inside the cabin is zero.

Solution procedure

Using the principle of superposition (Carslaw and Jaeger, 1959; Ozisik, 1968; Powers, 2006), $C(x_2,t)$ can be redefined as:

$$C\left(x_2,t\right)=C_1\left(x_2\right)+C_2\left(x_2,t\right) \tag{A3}$$

For $t \le t_0$:

$$C_1 = A_{L_2} e^{m_1 x_2} + B_{L_2} e^{m_2 x_2} + C_{inlet} \tag{A4}$$

where:

$$B_{L_2} = \frac{\omega_2}{\omega_1-\omega_4} S_{\varphi 2} + \frac{\omega_3-\omega_5}{\omega_1-\omega_4} C_{inlet}$$

$$A_{L_2} = -\frac{\omega_2\omega_4}{\omega_1-\omega_4} S_{\varphi 2} + \frac{\omega_1\omega_5-\omega_4\omega_3}{\omega_1-\omega_4} C_{inlet}$$

$$\omega_1 = \frac{\left[-\Gamma m_2+\rho V_L\right]}{\left[-\Gamma m_1+\rho V_L\right]} \;\; ; \;\; \omega_2 = \frac{1}{\left[-\Gamma A_c m_1+\rho A_c V_L\right]} \;\; ; \;\; \omega_3 = -\frac{\rho V_L}{\left[-\Gamma m_1+\rho V_L\right]}$$

$$\omega_4 = \frac{\left[\Gamma m_2+\rho V_L\right]}{\left[\Gamma m_1+\rho V_L\right]} e^{(m_2-m_1)L_2} \;\; ; \;\; \omega_5 = -\frac{\rho V_L}{\left[\Gamma m_1+\rho V_L\right] e^{m_1 L_2}}$$

C_2 is solved using the method of separation of variables (Carslaw and Jaeger, 1959; Ozisik, 1968; Powers, 2006):

$$\begin{aligned} C_2\left(x_2,t\right) &= X(x_2)T(t) \\ &= a_0 e^{-\beta_0^2 t} + 2\sum_{n=1}^{\infty} a_n \cos\left(\alpha_n x_2\right) e^{-\beta_n^2 t} \quad \text{if } V_L = 0 \\ &= 2\, e^{\frac{V_L}{2D}} \sum_{n=1}^{\infty} a_n \cos\left(\alpha_n x_2\right) e^{-\beta_n^2 t} \quad \text{if } V_L \neq 0 \end{aligned} \tag{A5}$$

where:

If $V_L = 0$:

$$\alpha_n = \frac{n\pi}{L_2} \;\; ; \;\; \beta_n{}^2 = \lambda + \alpha_n{}^2 D \;\; ; \;\; a_0 = \frac{1}{L_2}\int_0^{L_2} -C_1\left(x_2\right) dx_2 \;\; ; \;\; a_n = \frac{1}{L_2}\int_0^{L_2} -C_1\left(x_2\right)\cos\frac{n\pi x_2}{L_2}\, dx_2$$

If $V_L \neq 0$:

$$\alpha_n \cot(\alpha_n L_2) - \frac{D}{2V_L}\alpha_n{}^2 + \frac{V_L}{2D} = 0 \;\; ; \;\; \beta_n{}^2 = \lambda + \alpha_n{}^2 D + \frac{V_L{}^2}{4D} \quad (\alpha_n > 0)$$

$$[a_n]_{1\le n\le\infty} = [R_m]_{1\le m\le\infty}\left[L_{m,n}\right]^{-1}_{1\le m,n\le\infty}$$

$$R_m = \int_0^{L_2} -C_1(x_2)\cos(\alpha_m x_2)\, dx_2$$

$$L_{m,n} = 2e^{\frac{V_L}{2D}}\int_0^{L_2}\cos(\alpha_m x_2)\cos(\alpha_n x_2)\, dx_2$$

Computing all the infinite coefficients (a_n) is not required. A stopping criterion for computing a_n can be set, based on the scale of contribution of the first and the nth term in the concentration expression using coefficients of $V_L = 0$, i.e:

$$\left|\frac{a_n\cos(\alpha_n x_2)e^{-\beta_n^2 t}}{a_1\cos(\alpha_1 x_2)e^{-\beta_1^2 t}}\right| \le \left|\frac{a_n}{a_1}\right| e^{-\left(\alpha_n^2-\alpha_1^2\right)Dt} \le \varepsilon \qquad \text{(A6)}$$

where ε is any predefined very small number. The trend of reduction of coefficients is similar for $V_L \neq 0$. The final contaminant concentrations for $t \le t_0$ are shown in Eq. 4a & 4b. The coefficients and eigen values are obtained similarly for the two domains except that the sign of terms having V_L gets changed for x_1 reference. Moreover, the value of contaminant concentrations at $x=L_1$ should be the same from the two expressions (4a & 4b), hence:

$$C_{x=L_1}^{x\le L_1} = C_{x=L_1}^{x\ge L_1} \qquad \text{(A7)}$$

Since the concentrations are functions of $S_{\varphi 1}$ and $S_{\varphi 2}$ (refer to Eq. 4a, 4b, A4 and A5), Eq. A7 gives another correlation between $S_{\varphi 1}$ and $S_{\varphi 2}$ along with Eq. A1. Solving A1 & A7 simultaneously will give $S_{\varphi 1}$ and $S_{\varphi 2}$. The boundary conditions for $t \ge t_0$, i.e. after the contaminant source stops releasing, are:

$$\left.\begin{aligned} -\Gamma A_c\frac{\partial C}{\partial x} + \rho A_c V_L C = 0 \;\; \text{at } x = 0 \\ -\Gamma A_c\frac{\partial C}{\partial x} - \rho A_c V_L C = 0 \;\; \text{at } x = L_1 + L_2 \end{aligned}\right\} \qquad \text{(A8)}$$

and the initial condition is the contaminant concentration at $t = t_0$. The governing contaminant transport equation is solved using a new reference time scale t_1 ($= t - t_0$). The contaminant concentration along the length of the cabin is shown in Eq. 6. A and B can be obtained from C_{inlet} (similar to Eq. A4). Thus for $t \ge t_0$:

If $V_L = 0$:

$$\alpha_m = \frac{m\pi}{L_1 + L_2} \;\; ; \;\; \beta_m{}^2 = \lambda + \alpha_m{}^2 D$$

$$b_0 = \frac{1}{L_1 + L_2} \int_0^{L_1+L_2} \left(C\left(x, \mathrm{t}_0\right) - C_{inlet}\left(\mathrm{t}_0\right) - Ae^{m_1 x} - Be^{m_2 x} \right) dx$$

$$b_m = \frac{1}{L_1 + L_2} \int_0^{L_1+L_2} \left(C\left(x, \mathrm{t}_0\right) - C_{inlet}\left(\mathrm{t}_0\right) - Ae^{m_1 x} - Be^{m_2 x} \right) \cos\frac{m\pi x}{L_1 + L_2} \; dx$$

If $V_L \neq 0$:

$$\alpha_m \cot\left[\alpha_m \left(L_1 + L_2\right)\right] - \frac{D}{2V_L}\alpha_m{}^2 + \frac{V_L}{2D} = 0 \;\; ; \;\; \beta_m{}^2 = \lambda + \alpha_m{}^2 D + \frac{V_L{}^2}{4D} \quad (\alpha_m > 0)$$

$$\left[b_m\right]_{1 \le m \le \infty} = \left[R_n\right]_{1 \le n \le \infty} \left[L_{n,m}\right]^{-1}_{1 \le n,m \le \infty}$$

$$R_n = \int_0^{L_1+L_2} \left(C\left(x, \mathrm{t}_0\right) - C_{inlet}\left(\mathrm{t}_0\right) - Ae^{m_1 x} - Be^{m_2 x} \right) \cos\left(\alpha_n x\right) \; dx$$

$$L_{n,m} = 2e^{\frac{V_L}{2D}} \int_0^{L_1+L_2} \cos\left(\alpha_n x\right) \cos\left(\alpha_m x\right) \; dx$$